MEMBRANE FUSION IN A MODEL SYSTEM

Mucocyst Secretion in *Tetrahymena*

BIRGIT SATIR, CAROLINE SCHOOLEY, and PETER SATIR

From the Department of Physiology–Anatomy and the Electron Microscope Laboratory, University of California, Berkeley, California 94720

ABSTRACT

The freeze-fracture, freeze-etch technique can be employed to reveal new details of the process of fusion of two unit membranes For this study, mucocyst discharge in *Tetrahymena pyriformis* provides a model system with certain general implications The undischarged mature mucocyst is a saclike, membrane-bound, secretory vesicle containing crystalline material The organelle tip finds its way toward a special site, a rosette of 150 Å diameter particles within the plasma membrane. To match this site, the mucocyst membrane forms an annulus of 110 Å diameter particles, above whose inner edge the rosette particles sit. Discharge of some mucocysts is triggered by fixation. As discharge proceeds, the organelle becomes spherical and its content changes from crystalline to amorphous. The cytoplasm between the two matching membrane sites is squeezed away and the membranes fuse Steps in membrane reorganization can be reconstructed from changes in rosette appearance in the fracture faces. First, a depression in the rosette—the fusion pocket—forms. The rosette particles spread at the lip as the pocket deepens and enlarges from 60 to 200 nm. The annulus particles then become visible at the lip, indicating completed fusion of the A fracture faces of mucocyst and plasma membranes The remaining B faces of the two membranes have opposite polarities When the content of the mucocyst is released, the edges of these faces join so that the unit membrane runs uninterruptedly around the lip and into the pocket.

INTRODUCTION

The mechanism of membrane fusion has been an important but relatively intractable problem in cell biology for many years One primary difficulty in understanding fusion stems from the concept of the unit membrane (Robertson, 1959, 1972). A unit membrane must clearly undergo topological rearrangement to admit incorporation of additional foreign membrane, since its trilaminar structure requires a precise layer-by-layer matching of the two partners. This must add a high degree of spatial and temporal stringency to the fusion process. A second difficulty lies in the requirement of fine-grained differentiation among small areas of unit membrane to provide local sites that accept or reject certain fusion partners. For example, del Castillo and Katz (1957) postulate that a collision between specific sites on the axon membrane and on the synaptic vesicle membrane is necessary for temporary fusion and neurotransmitter release at the motor end plate A third difficulty concerns the triggering of fusion.

Most knowledge concerning the sequence of events taking place during fusion has been ob-

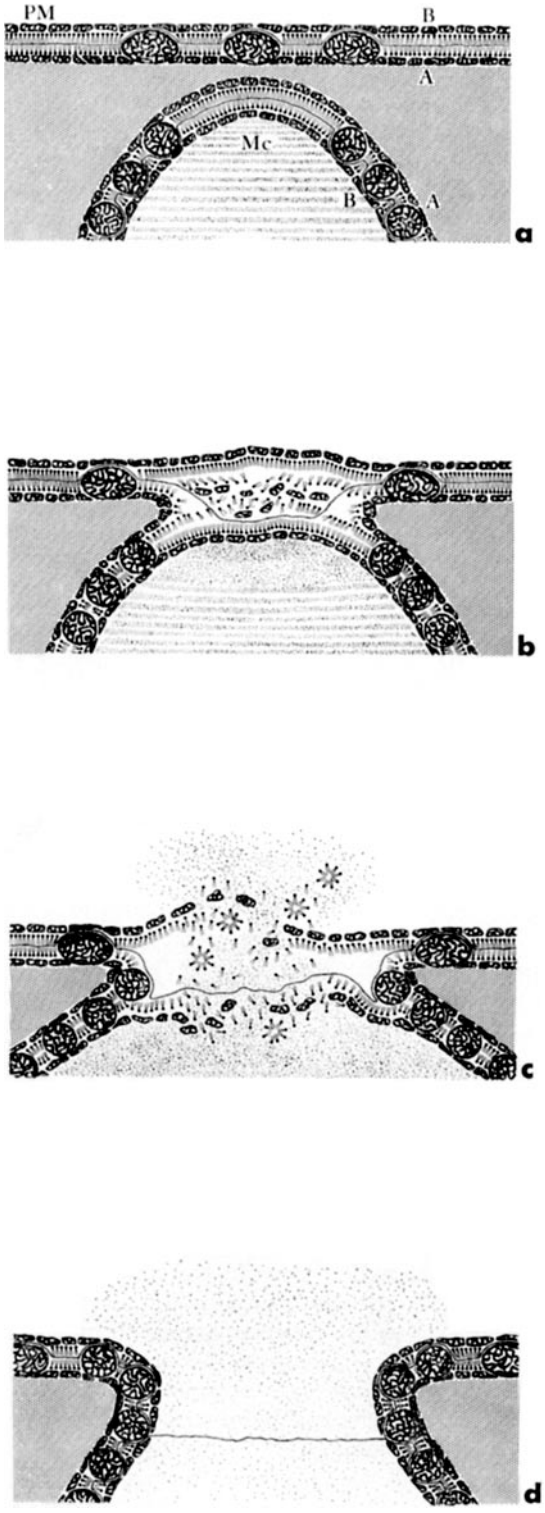

tained by morphological evidence. Aside from the description of the intricate relationship between intracellular membranes and of the flow of materials from one membrane-bounded compartment to another, a few workers, notably Palade and Bruns (1968), have attempted to examine the process of membrane fusion in conventional thin sections at high resolution Palade and Bruns have obtained images that show fusion of the endothelial cell unit membrane and underlying vesicles into a pentalaminar structure reminiscent of the fusion points of the tight junctions or of compact myelin However, such studies are hampered by section thickness, by lack of differential contrast in the membranes, and by a limited correlation between such images and local membrane chemistry These limitations are largely overcome by the freeze-fracture, freeze-etch technique. With the application of this technique to the problem of membrane fusion, an entirely new dimension emerges.

It has been convincingly demonstrated (Branton, 1966; Pinto da Silva and Branton, 1970; Tillack and Marchesi, 1970) that freeze-fracture produces a unique preferential split through membranes. The fracture produces two complementary halves of the membrane, the cytoplasmic half conventionally labeled A, the ex-

FIGURE 1 Interpretive diagram of membrane fusion during mucocyst discharge. (*a*) Cross-section of plasma membrane (*PM*) containing large rosette particles and underlying mucocyst membrane (*Mc*) containing rows of smaller annulus particles just before fusion. Wavy black lines indicate fractures that split the membranes into A and B halves. (*b*) Fusion begins when a hinge is formed between surface complexes corresponding to the rosette and the inner edge of the annulus. Wavy black line indicates fracture of the plasma membrane. Seen from face A, a nonetchable depression that corresponds to face B of the mucocyst membrane develops in the center of the rosette (compare Fig. 19 *b*) (*c*) When the rosette particles spread, evolution of the annulus results. Fusion of the A faces is completed. Wavy black line indicates fracture of the plasma membrane. Seen from face A, the depression in the center of the rosette corresponds to the expanding mucocyst content and reorganizing mucocyst membrane face B. This is now etchable (cf. Figs. 19 *f*, 21, and 22). (*d*) Reorganization is completed around the fusion lip. Fracture line now passes through expanding mucocyst content. See text for further explanation. Abbreviations are explained at the first appearance in the figures and are used consistently throughout.

terior half or its homologue conventionally labeled B (Fig 1) In model systems (Deamer and Branton, 1967) the plane of fracture has been shown to run through the middle of the hydrophobic lipid bilayer, thereby revealing internal membrane structure, while subsequent etching reveals true membrane surfaces In addition to this potential for examining fusion in *en face* views of both surfaces and interiors of partner membranes, freeze-fracture and freeze-etch techniques have been especially useful in defining within membranes local specialized sites of altered structure and of physiological significance such as cell junctions.

In an earlier short report (B Satir et al , 1972 *a*) we presented evidence to show that, during mucocyst discharge in the ciliated protozoan *Tetrahymena*, sites of membrane fusion can be pinpointed and that fusion can be followed in freeze-fracture replicas as it occurs within face A of the cell membrane A hypothesis of membrane reorganization during secretion was developed In this paper, we present a more detailed and extensive account of the series of events involved in membrane fusion in this system and additional evidence to clarify certain aspects of our hypothesis Some special features of membrane organization, including morphogenesis of the ciliary necklace in *Tetrahymena*, will also be illustrated and the general relevance to other biological systems will be discussed

Tetrahymena pyriformis (W) possesses an extremely well-organized, well-defined cortical membrane system which has been carefully described at an ultrastructural level by several workers (Pitelka, 1963; Tokuyasu and Scherbaum, 1965; Allen, 1967). The cilia and mucocysts are neatly arranged in rows The entire ciliated body is covered with a continuous plasma membrane (cell membrane) which includes the ciliary membrane Directly below the plasma membrane, a system of flat membrane-bound vesicles, the alveoli, is located. The alveoli, although connected to the plasma membrane via small fibers, do not interfere with analysis of the membrane events discussed here In the case of discharging mucocysts, all contact is made directly with the plasma membrane.

The process of mucocyst development and discharge has been studied in thin section by Tokuyasu and Scherbaum (1965) They suggest that the mucocyst develops from the endoplasmic reticulum. When the organelle is mature, it moves to a "rest" position under the plasma membrane and its content becomes crystalline During discharge, the crystalline pattern disappears and the mucocyst assumes a spherical configuration When discharge is triggered, the unit membrane of the mucocyst fuses with that of the cell.

MATERIALS AND METHODS

Conventional Transmission Electron Microscopy

Cultures of *Tetrahymena pyriformis* (W) were grown axenically on 2% proteose peptone at 26°C for 20–50 h (mid- to late-log phase). The cells were harvested by centrifugation in an International refrigerated centrifuge PR-1, at 1500 rpm for 5 min at 4°C The cells were then fixed in 3% glutaraldehyde for 30 min, postfixed with 2% OsO_4 in 0 025 M phosphate buffer, pH 7.4 for an hour, and embedded for conventional transmission electron microscopy as described in B Satir and Dirksen (1971). Sections were cut on a Porter-Blum MT2 ultramicrotome and were normally silver-to-gold in interference color The sections were stained with uranyl acetate and lead citrate The electron micrographs were taken with a Siemens 1A or 101 electron microscope at 80 kV.

Freeze-Fracture, Freeze-Etch Technique

Cells used for the freeze-fracture, freeze-etch technique were harvested as described above. The samples were fixed for 15–20 min in 0.5% glutaraldehyde in 3–6 mM phosphate buffer, pH 7 0, at room temperature, and then transferred to 20% aqueous glycerol for 2 h or overnight. The cells were then frozen in Freon 22 at −150°C and stored at liquid nitrogen temperature The frozen samples were fractured in a Balzers apparatus at −115°C and a platinum-carbon replica of the fracture face was prepared, usually without etching. The replicas were cleaned in bleach for 20 min, which for *Tetrahymena* is sufficient to remove all remaining cell debris. The replicas were then washed in distilled H_2O and mounted on 300-mesh uncoated grids.

When etching was desired, cells were fixed as above, washed and frozen in distilled water, and never exposed to glycerol. Etching time for these samples was 5 min at −100°C. Measurements of particle sizes on freeze-fracture or freeze-etch replicas are uncorrected for shadowing angle and platinum deposition.

Scanning Electron Microscopy

Material for scanning electron microscopy (SEM) was prepared in collaboration with Dr. E R. Dirksen. The cells were harvested, fixed with 2% OsO_4 in 0.025 M phosphate buffer for 1 hr, and then dried by the critical point method using CO_2 or Freon 12 (Cohen et al., 1968). Scanning electron micrographs were taken with a Cambridge Stereoscan Mark IIa SEM at 20 kV. Polaroid 55 P/N film was used to obtain SEM negatives.[1]

RESULTS

Scanning Electron Microscopy of the Surface

The topography of the outer surface of *Tetrahymena* is demonstrated in a scanning electron micrograph of the cell (Fig. 2). The outer surface consists of ridges and grooves and orderly rows of cilia can be seen, arranged along the primary (1°) meridians, running from the anterior to the posterior end of the cell. Cilia are found in several bend positions in grooves of the surface to the right of the ridges. In between the 1° meridians, the secondary (2°) meridians are located Several open pockets (circles) representing discharged or discharging mucocysts can be discerned. A circular rim or lip projects up from the surface and surrounds each pocket The outer diameter of the lip is about 200 nm. Mucocysts are found along both meridians. An asynchronous discharge of mucocysts is induced by brief fixation

Transmission Electron Microscopy

GENERAL ORIENTATION: A corresponding tangentially cut thin section of *Tetrahymena* is shown in Fig. 3. Cilia (Ci) are found in cross-section along one 1° meridian, above and below which lie two 2° meridians. Numerous cross-sections of mucocysts (Mc) are found in between adjacent cilia and along the 2° meridians. The mucocyst content varies from an electron-opaque crystalline array to a more electron-transparent amorphous mass. This is a reflection of different states of discharge.

Part of a longitudinally cut 1° meridian is seen in Fig. 4. Anterior and to the right of the cilium lies the parasomal sac (ps). This is a 79 nm diameter finger-like invagination which opens up to the exterior at the base of the cilium Its length is about 133 nm Cilia and parasomal sacs serve as important markers for orientation on the replicated surfaces.

MUCOCYST STRUCTURE AND SEQUENCE OF FUSION: The general morphology of the mucocyst as it approaches the plasma membrane is demonstrated in Figs. 6–8 The undischarged mature mucocyst is an elongated saclike structure of diameter 320 nm and length 930 nm, surrounded by its own complete 80 Å unit membrane. The end of the sac is rounded off into a hemisphere In this way, at the tip, a shallowly curved piece of mucocyst membrane comes to lie roughly parallel to the plasma membrane The mucocyst's tip finds its way up towards the plasma membrane, moving first to the meridian between two adjacent alveoli and then past the alveoli. A small portion of the mucocyst membrane approaches the underside of the cell membrane where the gap between the membranes is reduced to a few nanometers or obliterated entirely. Events between this stage and those in which fusion is complete (Fig 4) have proven difficult to reconstruct from thin sections

The crystalline material within the mature mucocyst before discharge is arranged with a longitudinal periodicity of about 180 Å. There are sometimes gaps, which may be bridged by fine fibers, between the relatively straight edges of the crystal and the membrane. As was previously noted by Tokuyasu and Scherbaum (1965), one of the first indications that fusion is occurring is a change in mucocyst content from this crystalline array to an amorphous mass. This is followed by a change of mucocyst shape from an elongate sac to a sphere of a diameter of 720 nm (Table I). In Fig. 4 the actual fusion of the two membranes has been completed. The accompanying shape and content changes are apparent. Discharge is well underway. The dissolving content of the mucocyst, now more than double its original volume, overflows into the medium. Except at the fusion aperture, the mucocyst membrane appears intact. Despite the almost explosive discharge of the content, reorganization of the membrane is highly localized; obvious fragmentation or dissolution is absent The fusion aperture widens to 245 nm in diameter as discharge occurs. The fused membranes form a 49 nm thick lip around the aperture, which is plugged by the discharging content.

[1] We thank Dr. T. Everhart for the use of SEM facilities.

FIGURE 2 Scanning electron micrograph illustrating the surface topography of the cell. Cilia are aligned along the primary (1°) meridians and open mucocyst pores (circles) can be discerned along the secondary meridians (2°). × 15,000.

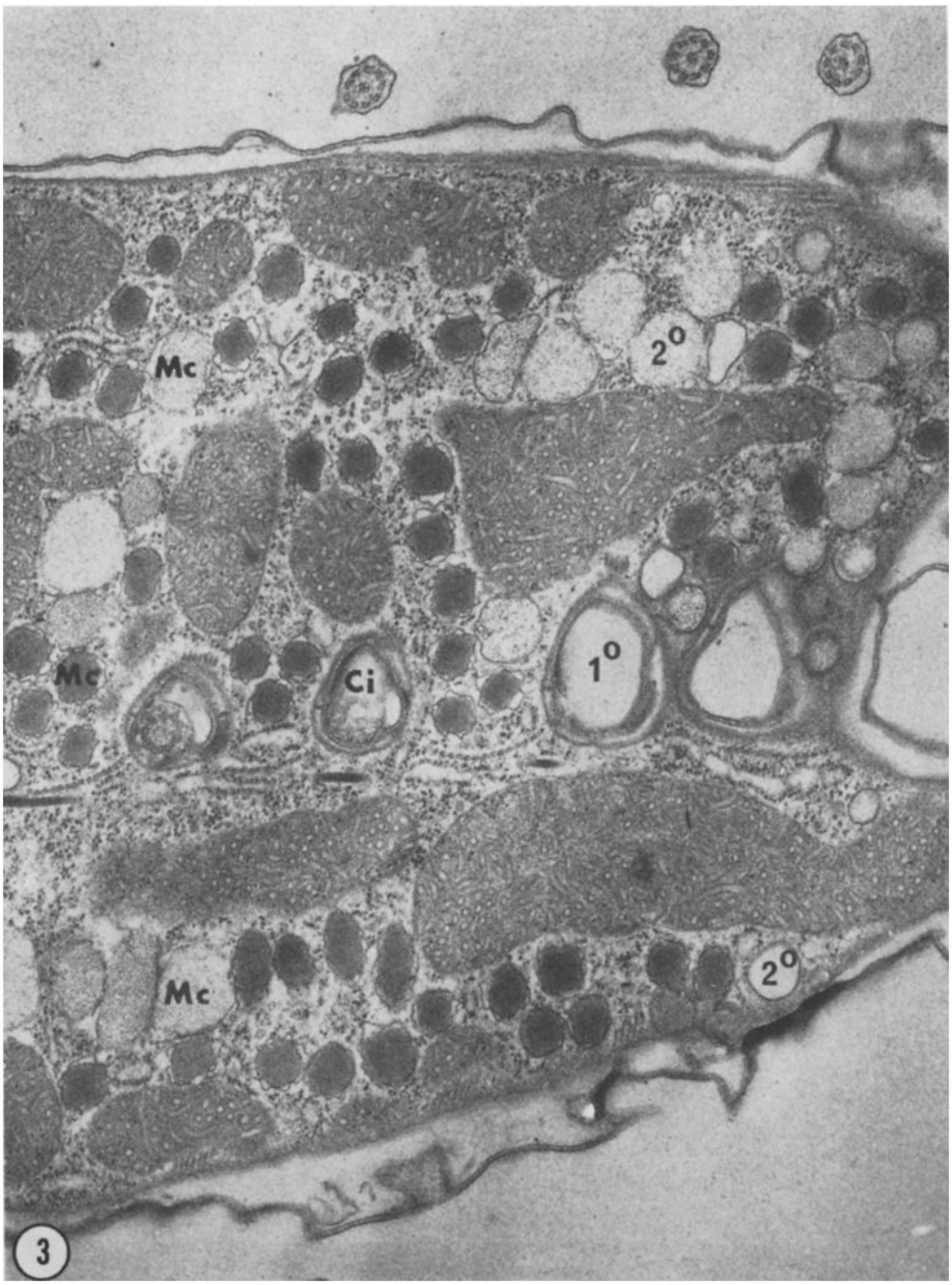

FIGURE 3 Tangentially cut thin section of *Tetrahymena*, illustrating one 1° meridian and two 2° meridians. Cilia (*Ci*) are found in cross-section along the 1° meridian Along the 2° meridians and in between cilia, numerous mucocysts (*Mc*) are present. Note differences in electron opacity of content in various mucocysts. × 24,000.

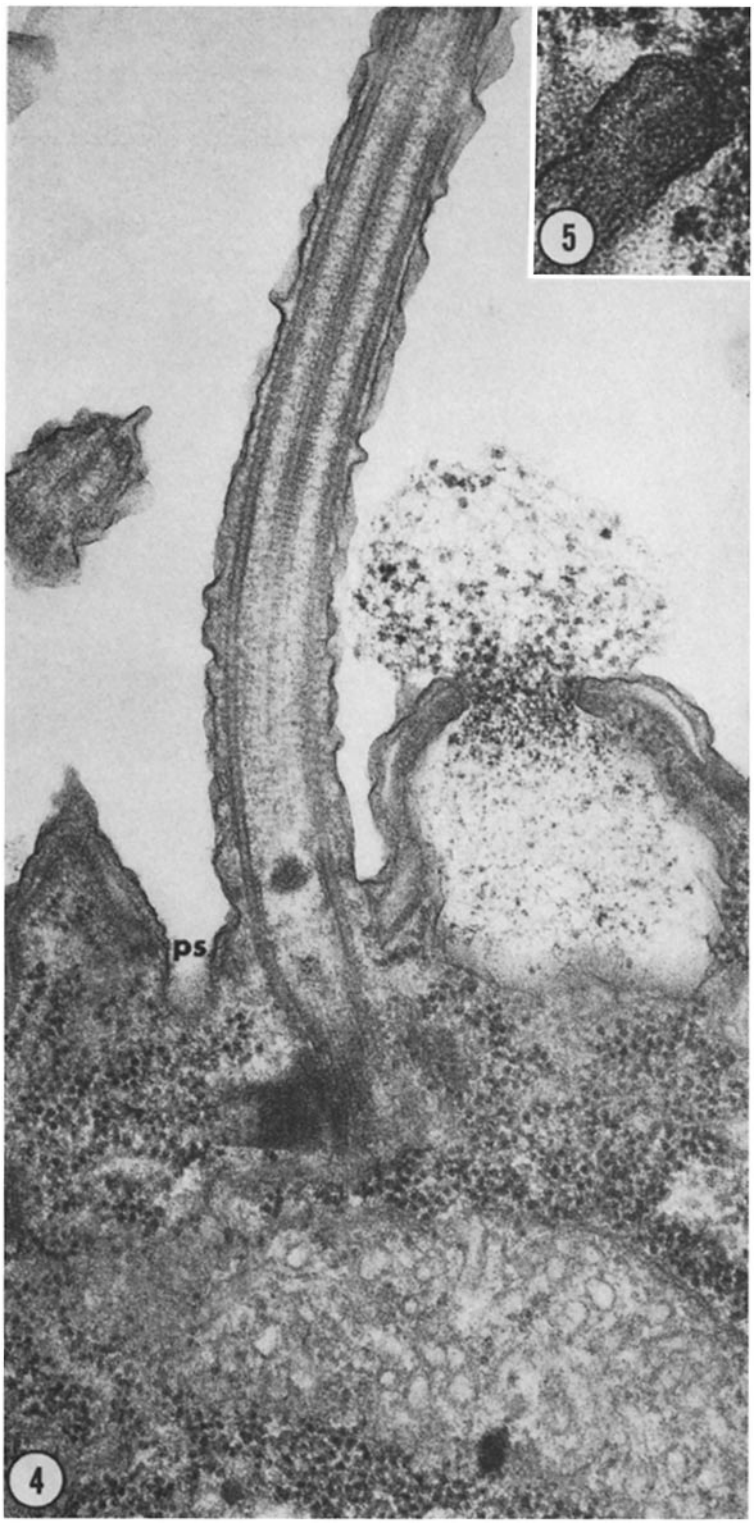

FIGURE 4 Longitudinal section through part of a 1° meridian showing a cilium, its accompanying parasomal sac (*ps*), and a discharging mucocyst. × 72,000.

FIGURE 5 Detail of fusion lip during mucocyst discharge showing the continuity of the strata of the unit membrane running from the mucocyst to the plasma membrane. × 216,000.

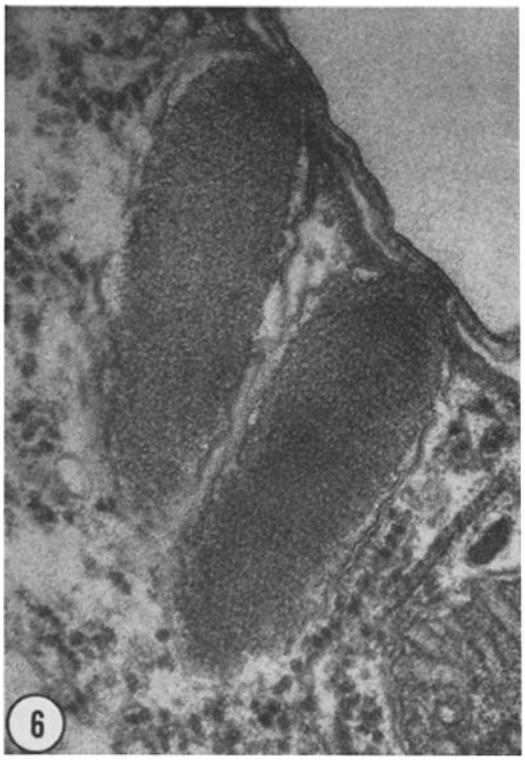

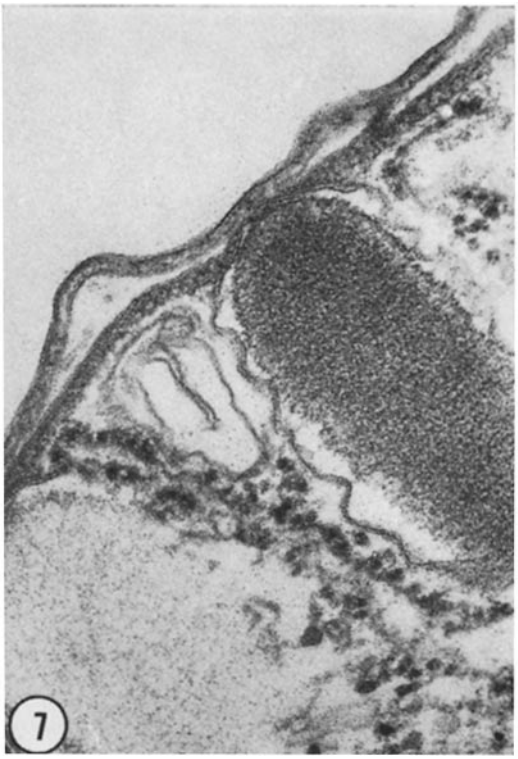

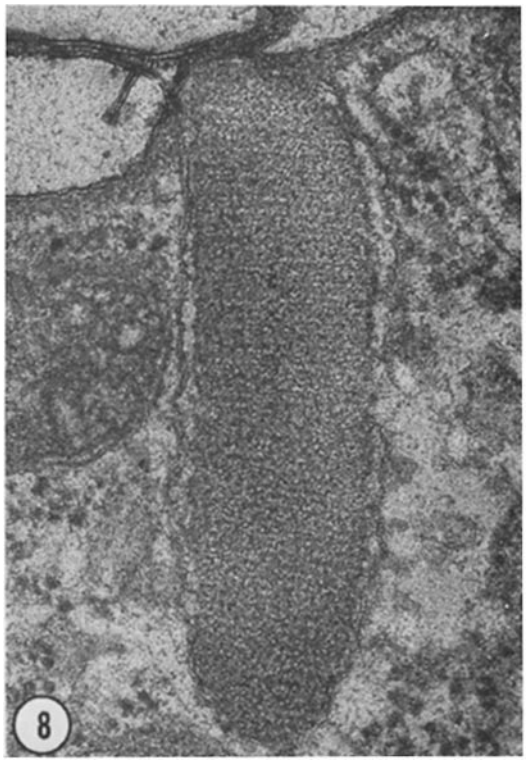

FIGURES 6–8 Mucocysts before discharge. Note sac shape and crystalline content. This series demonstrates how the mucocyst pushes its way up in between two adjacent alveoli to make direct contact with the plasma membrane. × 72,000.

TABLE I

Comparison of Undischarged Versus Discharged Mucocysts

	Undischarged	Discharged
Form	Elongate sac*	Sphere
Content	Crystalline	Amorphous
r (nm)	160	360
ht (nm)	610	—

* Approximately a cylinder of height (ht) and radius (r) capped by hemispheres of radius (r). Measurements are averages from at least five organelles, with average error $< \pm 15\%$

At the points of fusion, the mucocyst membrane evolutes and joins the plasma membrane The unit membrane appearance, with each lamella of the two conjoined membranes in register, continues without interruption around this juncture (Fig 5). Stages where the content is completely discharged are rarely observed in thin section Empty membrane pockets with openings of up to 96 nm and somewhat less depth than the discharging mucocyst are probably the remains of organelles that have been secreted at some previous time.

Freeze-Fracture

ARRANGEMENT OF CORTICAL ORGANELLES: The general appearance of the cortical organelles and plasma membrane of a freeze-fractured *Tetrahymena* is shown in Fig 9. A cilium has been fractured along its membrane revealing fracture face A (Ci_A). Three mucocysts are present, in all cases illustrating fracture faces B of their membranes (Mc_B). Close to a mucocyst, a mitochondrion (Mit) is shown cut in cross-fracture; these organelles rarely fracture along their membrane faces Several smaller vesicles are found in the otherwise relatively homogeneous cytoplasm.

A freeze-fracture image of the plasma membrane comparable to the thin section electron micrograph of Fig. 3 is shown in Fig. 10 The cell is viewed from the outside looking toward the cytoplasm, revealing an extensive fracture face A of the plasma membrane (PM_A). 1° and 2° meridians are easily recognized in such fractures. Along 1° meridians, the membrane fracture face is interrupted at intervals by cilia and their accompanying parasomal sacs. The parasomal sacs are located at the bottoms of depressions, from the centers of which the cilia rise upward. 2° meridians are well defined by straight or zig-zag orderly rows of rosettes (arrows). These rosettes are also present in between cilia along the 1° meridians Impressions stemming from the alveolar system (Alv) should be noted The meridians lie between separate alveolar cisternae.

FRACTURE FACES OF THE PLASMA AND CILIARY MEMBRANES: Both fracture faces of the plasma membrane of *Tetrahymena* have been examined in some detail Fracture face A (Fig 10) contains a background population of numerous randomly arranged 80–90 Å diameter particles, while fracture face B (Fig 11) contains fewer particles and some depressions With respect to their major topographical markers, such as cilia and parasomal sacs, the two fracture faces are complementary so that elevations on fracture face A appear as valleys on fracture face B and vice versa. 1° and 2° meridians are easily defined on fracture face B (Fig 11) From face B, the parasomal sacs protrude up toward the observer, and the cilia grow downward from the center of a plateau containing the sac Double replicas from both sides of a single fracture have not yet been examined.

The ninefold symmetry of the basal body is not well preserved in most of these images. More distally, cross-fractures of the axoneme sometimes reveal the 9 + 2 pattern quite clearly. At the base of the cilium, within the membrane, a two-stranded necklace is present A more detailed description of this structure will appear elsewhere (B. Satir et al , 1972 *b*).

In places along 1° meridians where the parasomal sac is present, mature cilia should always be seen in cross-fracture; instead, in Figs. 12–14, the membrane fracture face is sometimes completely intact. We interpret these appearances as representing the initial stages of ciliary morphogenesis, since such areas of the fracture face are marked by complete or incomplete rings of particles (arrows) that represent the ciliary necklace It is sometimes difficult to discern the necklace, since it is composed of similarly sized particles to those of the background, but the layout of circles is unmistakable The accompanying plateaus or depressions are not completely defined before the necklace is reasonably complete. The bulge in the center of the necklace in frac-

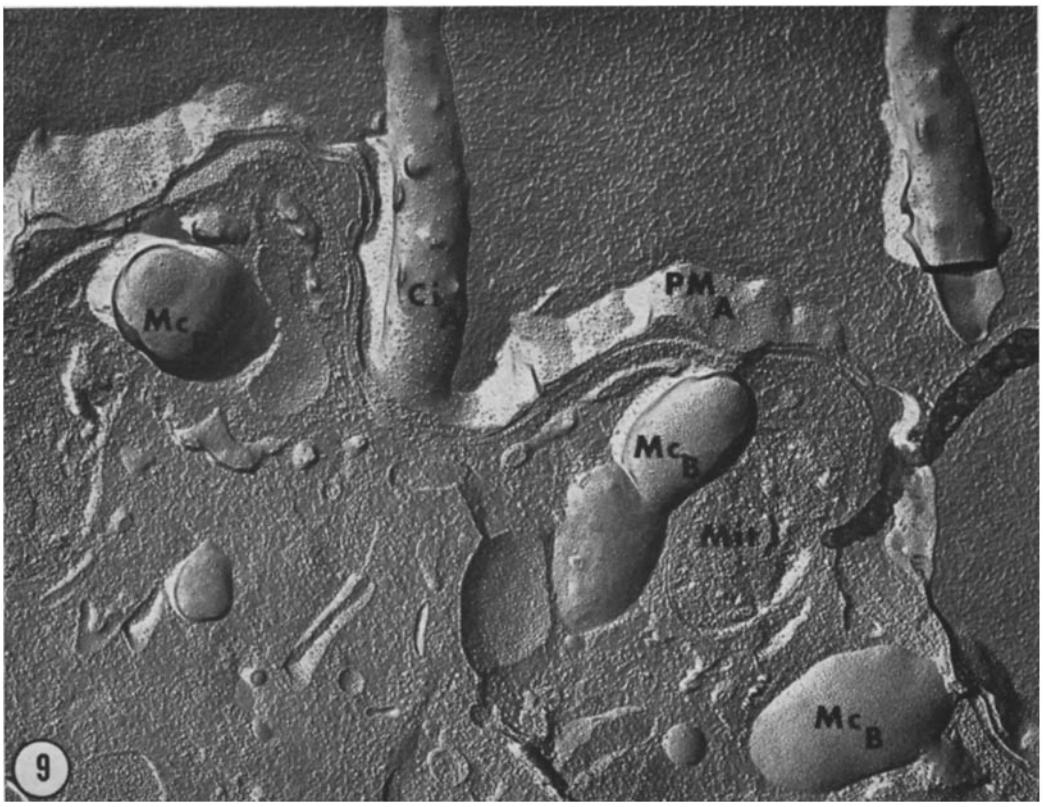

FIGURE 9 General view of a cross-fractured cell. The fracture plane has passed through the ciliary (Ci_A) and plasma membranes (PM_A) revealing face A. It then cuts across the cytoplasm and runs along several mucocyst membrane B faces (Mc_B). A mitochondrion (Mit) can be seen in cross-fracture. × 42,000.

ture face A (Fig. 12) represents the tip of the ciliary membrane at this stage, here some additional particles appear; a complementary image is seen on the B fracture face (Fig 14).

Although we cannot rule out the possibility that this appearance indicates ciliary resorption, cilia are known to be added as single units along the cortical rows of protozoa at irregular intervals throughout the cell cycle (Williams and Scherbaum, 1959; Nanney, 1971) and this should be occurring in these preparations Evidently, the site of growth is marked first by the appearance of the parasomal sac, which is followed in sequence by the organization of the ciliary necklace, the appearance of the depression in which the cilium sits, and finally outgrowth of the ciliary membrane The necklace is added one strand at a time.

THE ALVEOLAR MEMBRANES: Fractures of the alveolar membranes are seen in Figs. 14 and 15. Preliminary reconstruction suggests that fracture face A of this membrane has an inhomogeneous particle distribution. It is sparsely particulate when apposed to the plasma membrane (Alv'_A) (Fig 14), but heavily particulate at its basal side (Alv''_A) (Fig. 15). Fracture face B of the alveolar membrane (Alv'_B) near the plasma membrane correspondingly shows few depressions (Fig. 15). Cross-fractures through the alveolar content yield smooth profiles similar to those of the extracellular background.

THE ROSETTE: SITE OF MUCOCYST FUSION: A comparison between the distribution of mucocysts in thin sections of the cortex (Fig. 3) and the distribution of rosettes in fracture faces of the plasma membrane (Fig. 10) immediately suggests that the rosette marks the site of mucocyst discharge Counts of mature mucocyst profiles along a given length of 1° or 2° meridian usually approximate similar counts of rosettes.

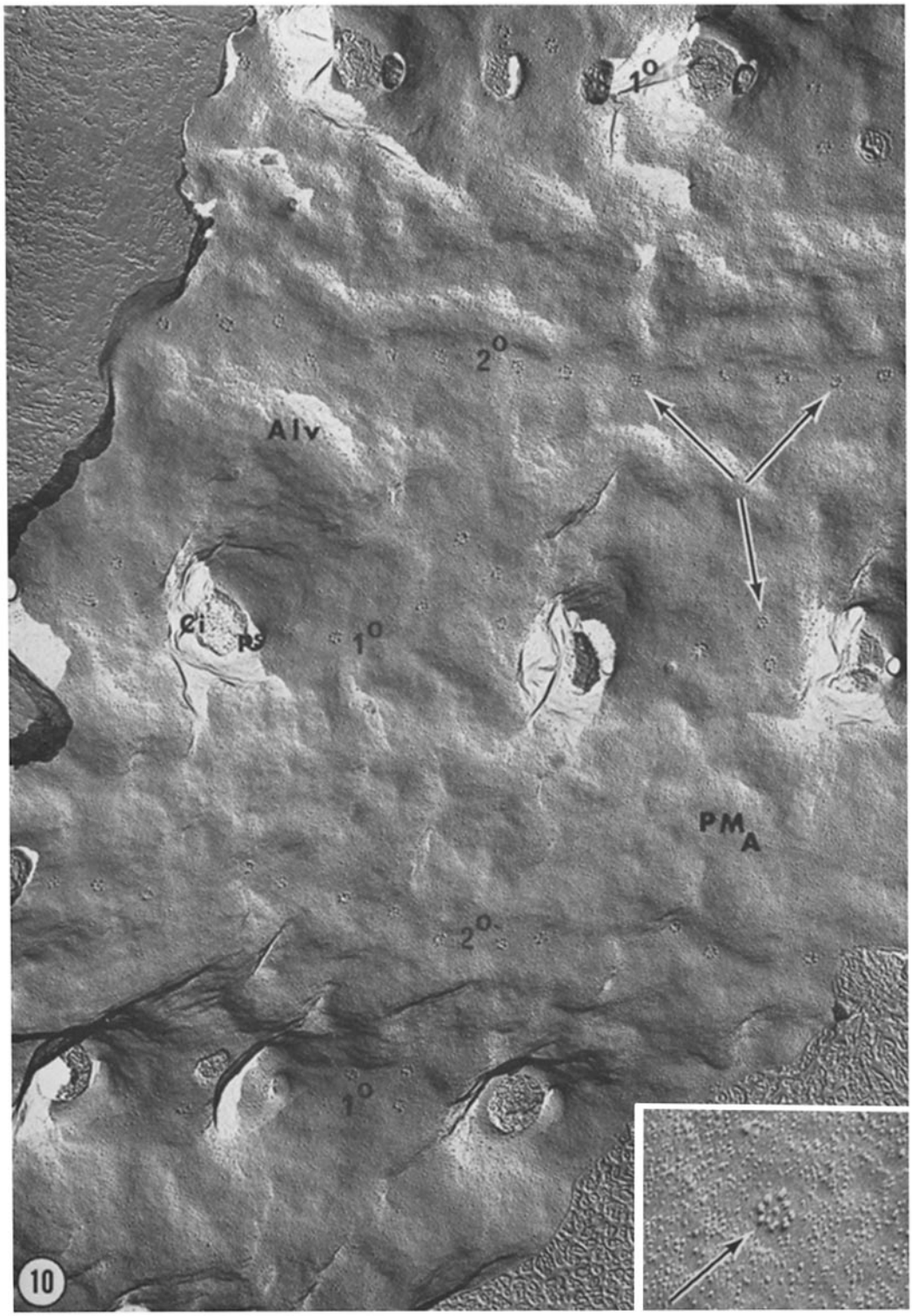

FIGURE 10 Fracture face A of the plasma membrane (PM_A) showing three 1° meridians and two 2° meridians Note underlying impressions of the alveolar cisternae (*Alv*) between meridians. Along the 1° meridians, cilia (*Ci*) and their accompanying parasomal sacs (*ps*) can be recognized in cross-fracture. Along the 2° meridians and in between cilia of the 1° meridians, rosettes of particles can be seen (arrows). × 18,000. *Inset:* high power of rosette (arrow). Note that some of the circumferential particles appear double. × 96,000.

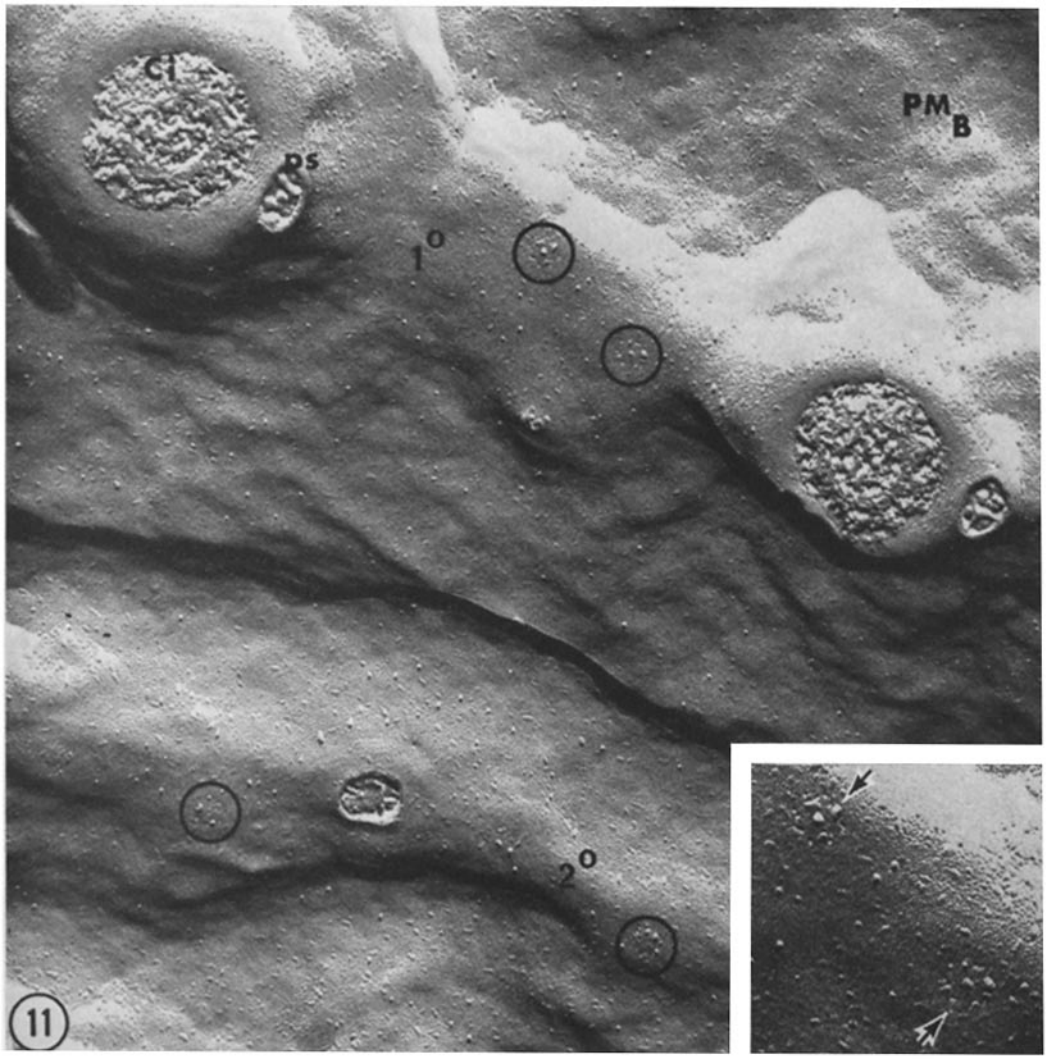

FIGURE 11 Fracture face B of the plasma membrane (PM_B). One 1° meridian and part of a 2° meridian are shown. Cilia (*Ci*) and parasomal sacs (*ps*) are found cross-fractured on raised plateaus. Along the 2° meridian and in between cilia, the B images of several rosettes (circles) can be discerned. × 72,000. *Insert:* high power of two B images of the rosettes (arrows). Note both center particles are present here. × 120,000.

Single rosettes can be seen at higher magnification on A fracture faces of the plasma membrane in Figs. 10 (insert) and 12 and on a B fracture face in Fig 11 (insert). The recognition of the B images of the rosettes is greatly aided by their meridional alignment.

On fracture face A, the rosette consists of 8–11 150 Å diameter particles evenly spaced around the circumference, with an occasional center particle. The inner diameter of the rosette is ca. 36 nm; the outer is then over 60 nm. The particles of the rosettes are larger than the background particles. Occasionally, the rosette particles seem to be comprised of several smaller particles (Fig. 10, insert). Few circumferential rosette particles follow fracture face B of the membrane (Table II) so that, on the B face, most of the circumference contains pits where the par-

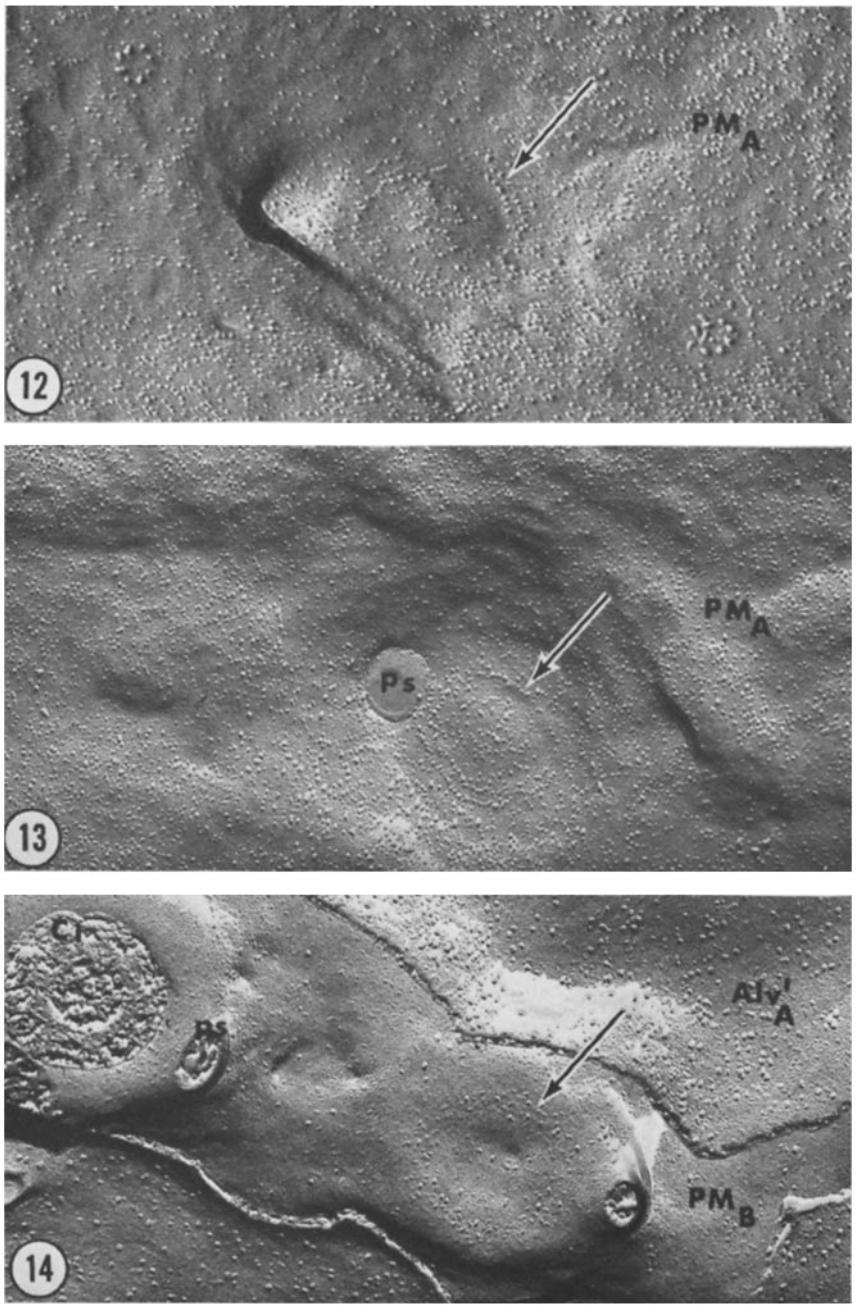

FIGURES 12–13 Fracture face A of the plasma membrane illustrating the formation of the ciliary necklace (arrows) before growth of a new cilium. Fig. 12, × 96,000; Fig. 13, × 72,000.

FIGURE 14 Fracture face B of the plasma membrane (PM_B) containing the complementary image of the developing ciliary necklace (arrow) along a 1° meridian. Note the neighboring "mature" cilium in cross-fracture and the A face of the alveolar membrane adjacent to the plasma membrane (Alv'_A) × 72,000.

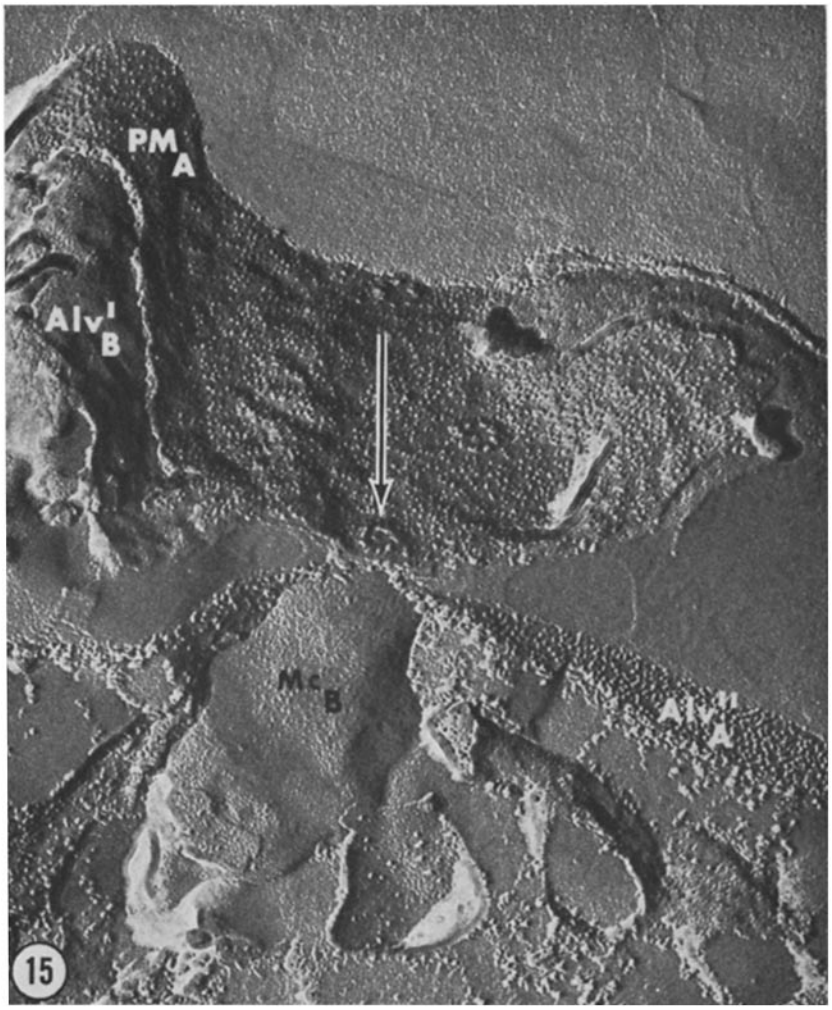

FIGURE 15 The mucocyst (Mc_B) in position, directly below one of the rosettes of the plasma membrane (arrow). Note the alveolar membranes Alv'_B and Alv''_A; the latter is heavily particulate. × 96,000.

ticles have been pulled out during the fracture However, in about half of the rosettes, the center particle adheres to fracture face B (Table II).

The actual point of contact between a mucocyst and a single rosette within the plasma membrane is shown in Fig 15. The fracture here passes through part of the plasma membrane and then continues along the mucocyst and alveolar membranes and through the cytoplasm, yielding an image comparable to the thin section images of Figs. 6–8 This pinpoints the mucocyst's position in regard to the plasma membrane rosettes. one mucocyst is found directly below one rosette. The initial point of contact between the tip of the mature mucocyst and the plasma membrane is at the rosette.

TABLE II

Fracture Face Partition of Rosette Particles

Fracture face	No. of circumferential particles/rosette	No of center particles/rosette	Total no of rosettes counted
A	8.2	0 5	20
B	1.1	0 4	18
A + B	9.3	0.9	—

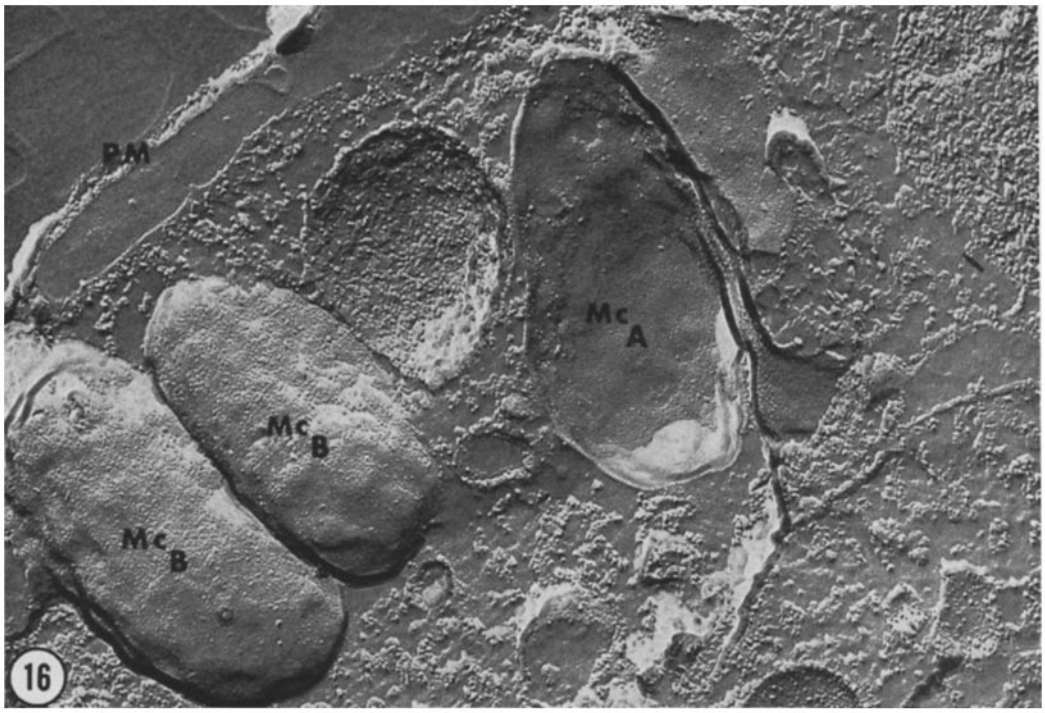

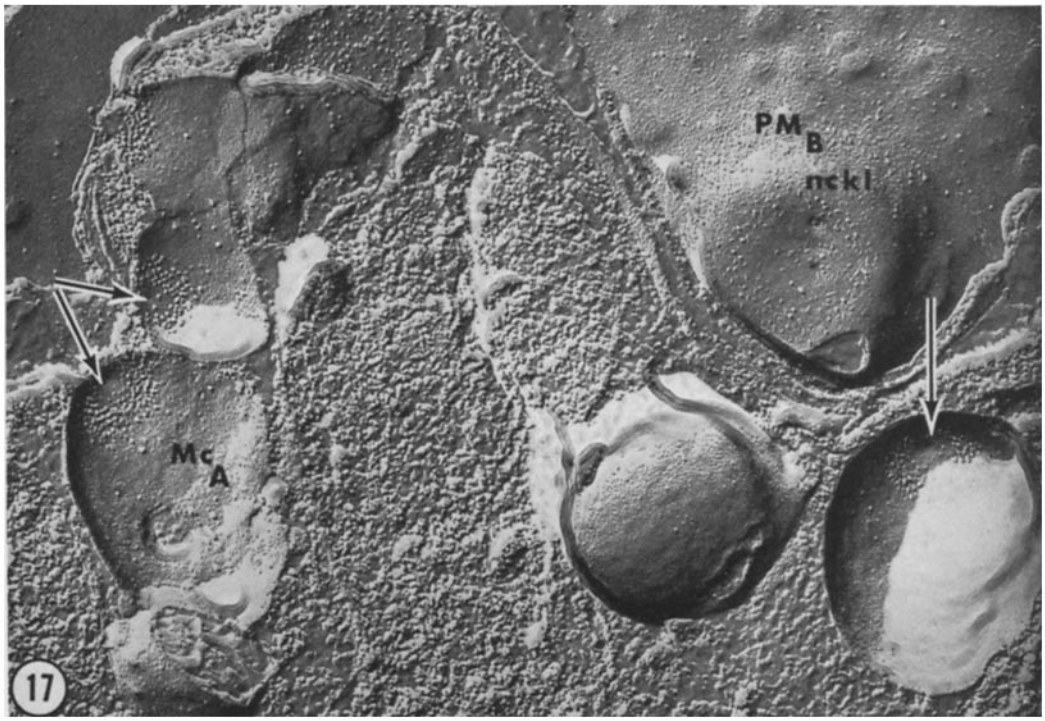

FIGURE 16 A (Mc_A) and B (Mc_B) face images of mucocysts far from the plasma membrane (PM), before contact. × 72,000.

FIGURE 17 After contact with the plasma membrane, all mucocysts A faces (Mc_A) display an annulus of particles. Arrows point to the smooth area, devoid of particles, within the annulus. On fracture face B of the plasma membrane (PM_B), a B face image of the ciliary necklace (*nckl*) can be seen. × 72,000.

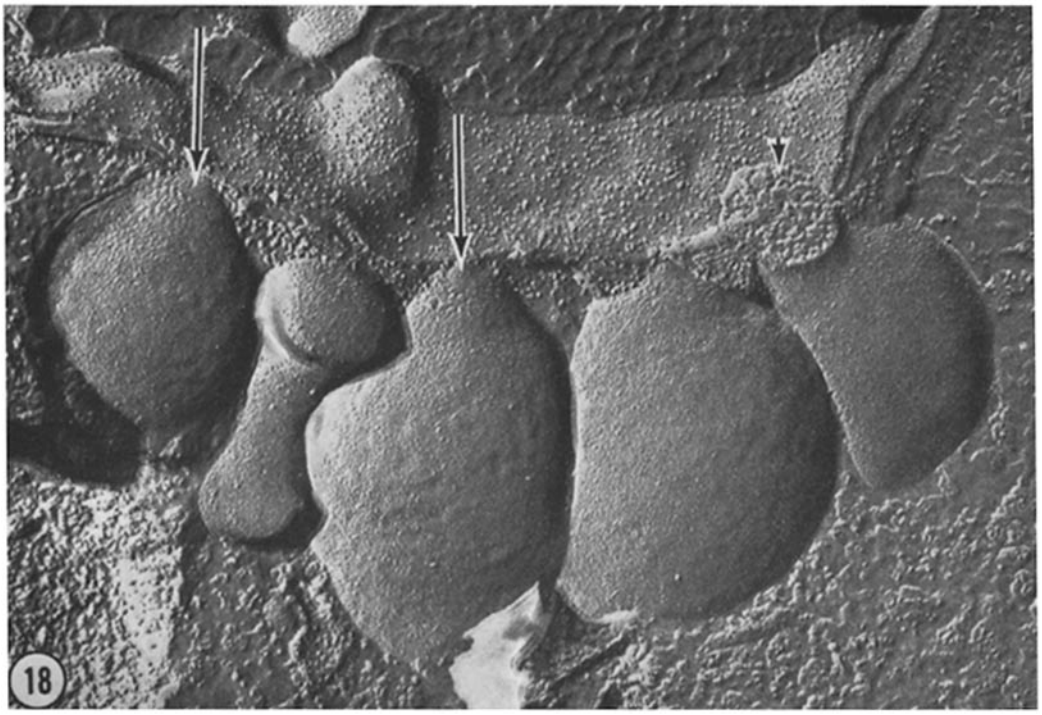

FIGURE 18 B face image of the annulus. Arrows point to the smooth central area at the mucocyst tip below which the fine imprint of the annulus can be discerned. Annulus particles generally do not adhere to the B fracture face. Arrowhead indicates fracture that has cut across content of discharging mucocyst. × 82,000.

THE MUCOCYST MEMBRANE: Fracture faces A and B of individual mucocyst membranes before contact with the plasma membrane are relatively smooth (Fig. 16). Very few scattered particles are present, even on fracture face A (Mc_A) near the mucocyst tip However, as the undischarged mucocyst comes within a critical distance of the plasma membrane, a change takes place (Fig. 17). This is especially obvious on fracture face A, where a 68 nm wide annulus, composed of five to seven rows of closely packed, ca. 110 Å diameter particles now appears within the membrane, in a position where the fusion lip will later form.

Correspondingly, a shallow imprint of the annulus appears as a series of depressions on fracture face B (Fig 18) All the annulus particles follow fracture face A. At the extreme tip of the mucocyst, a circular piece of membrane, diameter 61 nm, remains devoid of particles. It seems likely that the rosette of the plasma membrane fits over this circle.

SEQUENCE OF DISCHARGE: Careful observation of plasma membrane fractures, particularly along 2° meridians, reveals changed appearances of certain rosettes. These correspond to discharging mucocysts. In regions where different stages of the discharge have been preserved, the process of membrane fusion between a mucocyst and a single rosette of the plasma membrane can be reconstructed from fracture faces A and B of the plasma membrane. Such sequences are shown in Figs. 19 and 20.

It has also been shown above that the intact ~60 nm diameter rosette lies above an undischarged mature mucocyst and that its edge fits against the inner circumference of the mucocyst membrane annulus. On fracture face A, the first recognizable state in the fusion process is the appearance of a depression within the rosette to produce the fusion pocket (Fig 19 *b*) As fusion progresses, the diameter of the pocket increases from ca. 60 nm to approximately 200 nm. As this fusion aperture enlarges, the bigger particles of

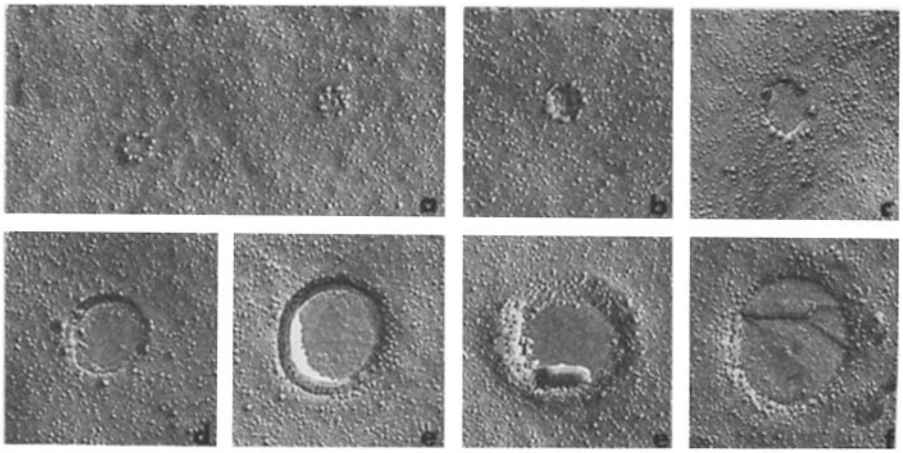

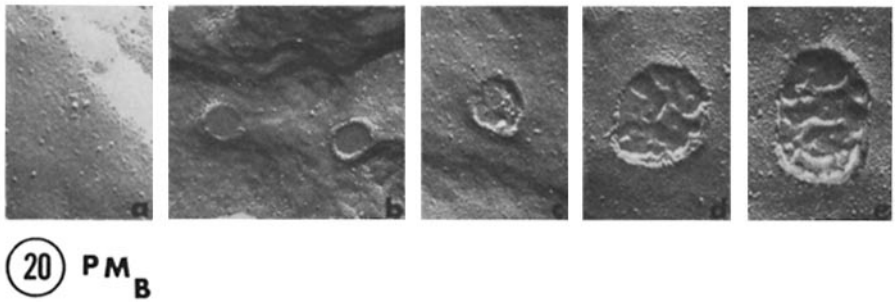

FIGURE 19 Reconstruction of the fusion process as seen from within the plasma membrane fracture face A. (*a*) Formation of sites: the rosettes before fusion. (*b*) First stage in fusion process a depression appears within the rosette. (*c*) The depression pocket widens: the particles of the rosette separate at the edge of the pocket. (*d*) Further separation of rosette particles and a deepening of the pocket (*e*) The particles of the annulus become visible. (*f*) Different depths can sometimes be seen within one fracture of the bottom of the pocket. × 72,000.

FIGURE 20 Fusion series seen from fracture face B. (*a*) The B image of a mature rosette. (*b*) The pocket aperture widens. (*c–e*) The pocket opens to the exterior and the fracture goes through the mucocyst content. × 72,000.

the rosette become separated at the lip of the pocket (Fig. 19 *c, d*) The pocket deepens. Finally, the particles of the annulus become clearly visible at the lip (Fig 19 *e, f*). At the bottom of the pocket, the fracture face is usually smooth throughout. Sometimes, several depths of fracture can be seen within a single pocket (Fig 19 *f*)

The markers are not as obvious on fracture face B, but the fusion process can still be followed (Fig. 20). As fusion begins, the B face imprint of the rosette is replaced by an elevated ridge (Fig 20 *b*). At this stage, although the fusion aperture has widened to ca. 80 nm, the fracture face remains unbroken As the aperture enlarges further, the character of the central area changes and eutectic ridges appear Now (Fig. 20 *c, d, e*) the fracture clearly passes through the discharging mucocyst content (cf Fig 18, arrowhead) and the opening to the exterior has been completed.

Freeze-Etching of the Fusion Pocket

After 5 min of etching of appropriate non-glycerol-treated cells, ice sublimation exposes the surface of the plasma membrane (PM_S) (Fig 21). Mucocyst fusion pockets are sometimes revealed both on a fracture face and on the plasma membrane surface in the same replica. In an opening pocket, there is an obvious height step between the edge of the surface (etch face) and fracture face A (Fig 21, arrow). The particles of the annulus are clearly visible on fracture face A; they approximately match the edge of the etch face in height, but they are not visible on the surface itself. Therefore, after fusion, the annulus particles must traverse the greater part, but not the entire thickness, of the plasma membrane. Impressions of the rosettes before fusion are sometimes seen on the cell surface after etching, but again, the rosette particles are not seen.

In Fig. 21, the etch face extends down into the pocket and continues across the exposed bottom of the pocket itself At the right side of the pocket, fracture face B of the mucocyst membrane is visible as a thin dark crescent adjacent to fracture face A The appearance of these two adjacent fracture faces is typical of single fractured membranes, as shown by Branton (1966). To the left, fracture face B is also continuous with the etch face at the bottom of the pocket. Thus, this pocket bottom probably represents a stage in reorganization where the outer plasma membrane surface is continuous with part of the mucocyst B fracture face as represented in the diagram of Fig 1 *c*

Pocket bottoms of smaller diameter viewed from fracture face A (Figs. 21 and 22) are not etchable, that is, their appearances do not change upon etching. However, pockets of larger diameter are etchable Particularly, pits and holes appear in the replica on these bottoms. Holes also appear within large pockets in fracture face B of the plasma membrane in etched preparations, although along the same meridian, rosette sites remain intact (Fig. 23)

DISCUSSION

In this paper we have demonstrated a sequence of events taking place before and during fusion of mucocyst and plasma membranes in *Tetrahymena* that involves the specific reorganization of both membrane interiors. Fig. 1 embodies several separable points of a hypothesis of the dynamic basis of this reorganization We shall discuss a number of distinct aspects of the fusion event: (*a*) formation of sites within the plasma membrane, (*b*) rearrangement of the mucocyst membrane, (*c*) fusion, rupture of the two membranes, and discharge. Finally, we shall consider the general implications of our finding for membrane fusion in other cells.

Formation of Sites within the Plasma Membrane

As have been amply demonstrated by others (Branton, 1966; Chalcroft and Bullivant, 1970; Wehrli et al, 1970), freeze-fracture splits membranes along a unique fracture plane to yield complementary fracture faces, here labeled A and B This complementarity is clearly illustrated by the rosettes in the *Tetrahymena* plasma membrane. The large circumferential particles of the rosette partition, so that upon fracture almost eight times as many adhere to the A rather than to the B face (Table I) The total number of particles (9) within the rosette circumference before fracture is given by the sum of the average number of particles on face A (8.2) plus the average number on face B (1.1). The central particle within the rosette is different from the circumferential particles in either position or affinity, so that it moves with the B face almost half of the time.

The rosette is a specialized and remarkable component of the *Tetrahymena* plasma membrane, which marks unequivocally the central point of mucocyst contact with the plasma membrane (Fig 15). The rosette is especially obvious, partly because of the unique geometry of mucocyst secretion, where fusion sites are confined to, and hence aligned along, the meridians between alveoli. In fracture faces, particles probably represent protein that penetrates into or traverses the hydrophobic portion of the membrane (Engstrom, 1970; Pinto da Silva, 1972) while the smooth background probably represents a continuous lipid matrix (Deamer et al., 1970). The rosettes then represent a highly ordered, inhomogeneous arrangement of molecules, probably protein aggregates, in this matrix. In this respect, the rosette is another example of localized structural arrangements of membranes that already includes cell junctions (Kreutziger, 1968; Gilula et al, 1970) and the ciliary necklace (Gilula and Satir, 1972; B. Satir et al, 1972 *a*, *b*). Like these, the rosette may provide specific

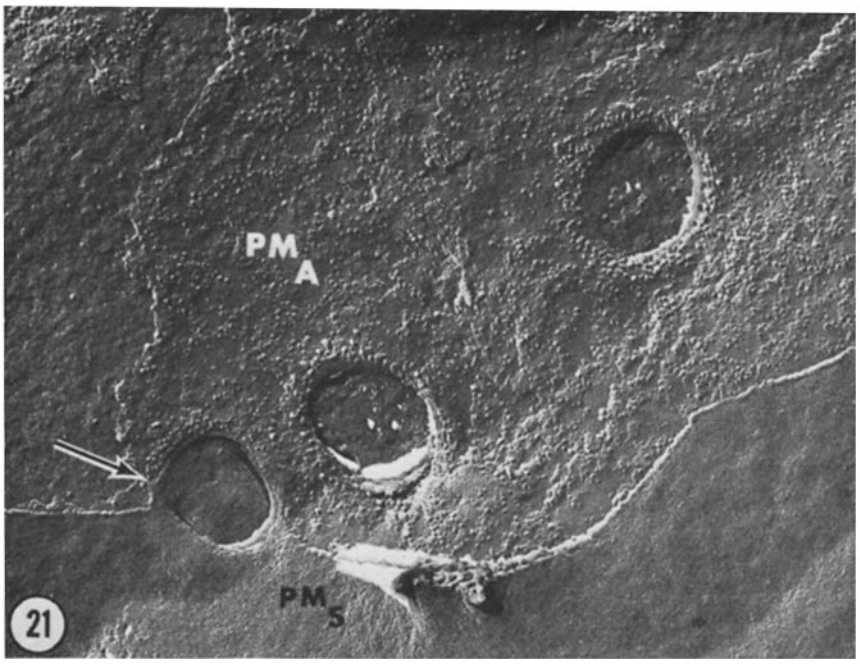

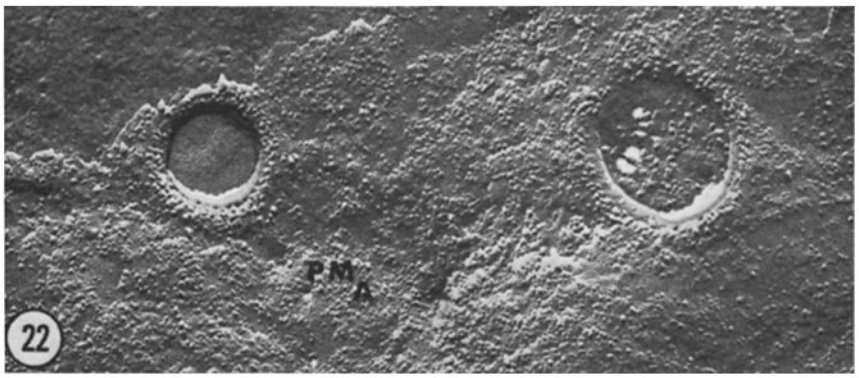

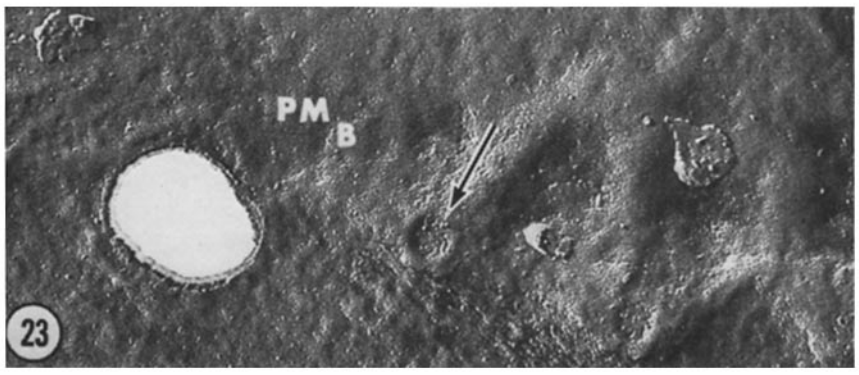

FIGURES 21–22 A face images of etched preparations In Fig 21, the outer surface of the plasma membrane (PM_S) is also revealed after 5 min of etching Note how the surface is continuous with the bottom of the pocket of a discharging mucocyst (arrow) On the fracture face, the particles of the annulus are clearly visible at the edges of the pockets. Note the holes and pits resulting from etching of the larger diameter pockets See text for further explanation. × 72,000

FIGURE 23 Fracture face B of the plasma membrane after 5 min of etching. The fracture has passed through an open mucocyst that leaves a hole in the replica after etching. Note the presence of an intact B image of a rosette (arrow). × 72,000.

channels for the movement of ions or small molecules through the membrane. It is noteworthy that several different particle aggregates, such as the rosette and the ciliary necklace, may occur at particular loci along a single membrane. In ciliates, such internal membrane differentiations may participate in a fundamental way in cortical patterning.

The 60 nm diameter rosette represents one, perhaps the initial, stage in rearrangement of the *Tetrahymena* plasma membrane for mucocyst fusion. The rosette is not a permanent site within the plasma membrane. When fusion actually occurs, the large rosette particles are separated further and further at the edge of the fusion pocket, finally to become lost or indistinguishable among the background particles. How the process of re-formation of these rosettes takes place cannot as yet be explained. Several possibilities are suggested: the large rosette particles may reappear (*a*) *de novo* as a result of new synthesis, (*b*) via a conformational change in an ever-present surface protein, (*c*) by a conglomeration of two or more of the less conspicuous background particles, or (*d*) by a combination of these processes. Certain images (Fig. 10, insert) suggest that smaller subunits comprise a rosette particle. Membrane fluidity (Frye and Edidin, 1970) provides a mechanism by which conglomeration can take place. Freeze-fracture particles can be made to aggregate by a variety of techniques, including pH and temperature changes (Engstrom, 1970; Pinto da Silva, 1972).

Our etching results at places where rosette particles should be seen (Fig. 21) provide some of the first evidence of particle height within the membrane The 150 Å diameter particles do not bulge above the membrane surface on etching. Such particles must be elliptical rather than spherical; their height probably approaches, but does not exceed, membrane thickness. Accordingly, we are able to detect 40 Å height deviations in the fracture plane as quite obvious particles.

Rosette formation is a necessary but not sufficient precursor to mucocyst discharge. It has been observed by several authors (Pitelka, 1963; Tokuyasu and Scherbaum, 1965) that mucocysts appear to rest below the plasma membrane awaiting a trigger to discharge. We suggest that at this time rosettes are already present, aiding the mucocysts in their final positioning, and perhaps also inducing formation of the annulus. Although the number of "mature" undischarged mucocysts corresponds to the number of rosettes, all do not discharge simultaneously when triggered.

Rearrangement of the Mucocyst Membrane

In the mucocyst membrane, the first obvious sign of impending discharge is the appearance of the annulus (Fig 17). The annulus is absent in mucocysts found at some distance from the plasma membrane (Fig. 16). Like the rosette, which is its partner in the process, the annulus appears before discharge as a necessary reorganization which does not in itself complete the preparation for fusion, so that all mucocysts with annuli underlying rosettes cannot be triggered to discharge.

The mechanism of mucocyst migration and maturation is not understood It may be that cortical microtubules or microfilaments are involved in positioning the mucocyst We suppose here that the annulus is induced when the mucocyst membrane comes within some critical distance of the plasma membrane site Formation of the annulus represents another example of a sudden appearance of particle arrays where none were seen before If the appearance of the array is the result of particle mobility in the plane of the membrane, it may be that particles from the entire membrane flow towards the anterior end of the organelle during the maturation period.

Fusion, Membrane Rupture, and Discharge

Very little is known about the actual trigger mechanism inducing membrane fusion and the following discharge. For the mucocyst, descriptions of this process, dating back to Bresslau (1921), demonstrate that discharge can be induced by addition of different stains or by pH and temperature changes. It is worth noting that the latter two are the same agents that are known to induce particle movement in the plane of the membrane in other systems Events from the triggering of fusion to the beginning of discharge take at most a few hundred milliseconds (Pitelka, 1963), and can at least partially be captured by glutaraldehyde fixation.

Full competence for fusion is likely to be a physiological as well as a topological event. Before fusion, the membranes can be thought of as

barriers to free flow of materials, including ions, from the mucocyst interior to the exterior As a consequence of these barriers, the mucocyst content remains in an insoluble paracrystalline form, although it is readily soluble in the external medium. A breach of the barriers might be effected by the formation of a small number of electrotonic junctions in the membranes. The apposition of particle-laden membrane regions separated by a narrow channel is morphologically reminiscent of junctions in other situations (Gilula et al , 1970). This postulation has several advantages, not the least of which is that known mechanisms can be invoked for most of the discharge process For example, junctional permeability is regulated by simple controls such as membrane potential, Ca^{++} concentration, etc. (Loewenstein, 1967). An alternative hypothesis would be that permeability depends on specific enzyme activation regulated by such controls.

Mature mucocysts could explode when membrane permeability increases so that ion changes within the mucocyst cause solubilization of the crystalline content. From conventional electron microscope evidence, the first sign of fusion is a change in electron opacity of the content from crystalline to amorphous Solubilization will eventually lead to an increase in osmotic pressure within the mucocyst, causing an influx of water.

Two steps accompany influx: (*a*) The membrane changes shape, from a sac to a sphere, which maximizes the volume that can be contained within the given membrane area. (*b*) When expansion reaches a critical value, a site-specific local rupture of the membrane occurs. One indication of this specificity is that, although rupture obviously interrupts the fracture faces of the fusion membranes, the interruption is always bounded by the particles of the rosette and mucocyst annulus The area occupied by the rupture is only about 2% of the total mucocyst membrane surface. Once rupture has been effected, the content can dissolve and diffuse away into the exterior without further hindrance. As the mucocyst content expands, it is likely that total mucocyst membrane area initially remains reasonably constant (Tokuyasu and Scherbaum, 1965). About a 20% increase in volume could be accommodated by the shape change without surface expansion However, our best measurements indicate that the mucocyst eventually swells to nearly three times its original volume so that the surface must increase by up to 70% (Table I). How this increase in membrane surface comes about is not clear Membrane stretching would involve major molecular changes over long distances and an eventual "thinning" of unit membrane dimensions and may be limited by such factors

As the cytoplasm is squeezed away, the first point of contact between mucocyst and plasma membrane is at the apposing cytoplasmic surfaces that lie directly above the center of the annulus and below the rosette (Fig 1 *a*). The center of the rosette fits neatly inside the annulus, so that the rosette particles lie in a ring just above the innermost rows of annulus particles. A single rosette occupies approximately 28×10^4 Å^2 of membrane surface If the rosette surface were comprised of globular proteins, on an average 60 Å in diameter, fusion would involve a maximum of about 100 protein molecules above the rosette, and a similar number above the annulus center. A likely possibility is that the rosette particles are internal extensions of surface protein or lipoprotein We propose that the initial interaction in membrane fusion involves bond formation to produce a hinge between the surface expressions corresponding to rosettes and those corresponding to the inner edge of the annulus (Fig 1 *b*)

The fusion trigger causes the rosette particles to spread. At the fused hinge, this spread produces evolution of the annulus particles (Fig. 1 *c*), which then appear in the same plane as the rosette particles (Fig. 1 *d*). In this way, fusion of the A fracture faces of the respective membranes takes place.

Fusion of A fracture faces precedes fusion of the B fracture faces Unbroken membrane fracture faces (essentially lipid monolayers) are, in general, not etchable both in theory and practice (Branton, 1966). In a face A fracture of the plasma membrane, we interpret the smooth, unchanging, appearance of the bottoms of fusion pockets of smaller (ca. 80 nm) diameter as unbroken B fracture faces of the mucocyst membranes (Fig 1 *b*). In support of this interpretation, the smaller diameter bottom fractures in Figs. 21 and 22 are not etched. Larger diameter pockets along the same meridians are etchable, having presumably reached the stage of Fig. 1 *c*, where the lipid monolayer is no longer intact Fig 19 *f* shows the appearance of these fractures before etching. Corresponding results are ob-

tained in face B fractures of the plasma membrane as the fusion aperture widens (Figs 20 and 23) The resultant half-membranes, corresponding respectively to fracture face B of mucocyst and cell membranes, have opposite polarities (Fig. 1 *b*) They now plug the fusion pocket and prevent rupture. Originally, these opposite B half-membranes are separated by a distance corresponding to the thickness of the fusing face A's. We are unable to give a detailed account of their fate at this time One possibility that we think likely is that the explosive expansion of volume that is occurring disperses some of these micelles in the medium (Fig. 1 *c*). Where dispersion does not occur, the two liberated half-membranes could approach each other and join at the lip. The number of molecules liberated by dispersion would in all events be reasonably small.

In a condensed 70% phospholipid–30% cholesterol monolayer, the average area per molecule is 65 Å^2 (Van Deenen, 1965). In the center of the annulus, a maximum of less than 10^4 phospholipids would be associated with each membrane fracture face A similar number would be associated with each half of the center of the rosette. Only a fraction of these and the associated surface proteins need be lost; in the most conservative hypothesis, this loss would approach zero.

When fusion and membrane reorganization is complete, fractures pass through the mucocyst content which is an aqueous suspension, and hence ice when frozen (Fig. 1 *d*) Upon etching, this will sublime, producing alterations in the fracture appearance and holes in the replica. In thin section, the unit membrane appearance continues uninterrupted from the plasma membrane around the lip and into the fusion pocket. In freeze-etch preparations, the surface of the membrane follows an identical uninterrupted course (Fig 21). Obviously, reorganization of the membrane surface occurs concurrently with the changes in the interior observed by freeze-fracture.

General Implications for Secretion in Other Cells

Although there has been considerable freeze-fracture study of cells where vesicle fusion with the plasma membrane should be commonplace, for example at synapses (Akert et al , 1969) or in capillary endothelium (Nickel and Grieshaber, 1969, Leak, 1971), detailed particle arrangements corresponding to those seen here have not yet been reported elsewhere Partly, interpretation has been hampered by previous controversy about the plane of membrane fracture, which now seems settled. Our results corroborate the suggestion of del Castillo and Katz (1957) that there must be specific matching sites on vesicle and cell membrane for fusion to take place In our laboratory, particle arrays corresponding to the rosette have been seen above secretory organelles in several protozoa. In *Paramecium aurelia*, a rosette is found above the center of the trichocyst (B. Satir and C. Schooley, in preparation), in a heliozoan (*Heliophrys marina*) rosettes appear in connection with the haptocyst (L. Davidson, personal communication). In a helioflagellate (*Ciliophrys marina*), above a haptocyst-like secretory vesicle, the site within the plasma membrane consists of a plaque of particles in a cubic array. The total number of rows and particles is variable (L. Davidson, personal communication). In *Paramecium*, the homologue of the annulus has also been identified In all these cases, as with *Tetrahymena*, the location of the secretory organelles and the timing of discharge is well defined. To our knowledge, no attempt has yet been made to synchronize secretion before freeze-fracturing with any metazoan cell system. Under more random physiological and topographical conditions, small particle arrays or rosettes on a particulate background could well be overlooked.

One particularly tempting generalization provided by our system is that the particle arrays represent molecular hydrophilic channels that permit ion flow In secretory vesicles, containing concentrated material, that are not spherical in shape, activation of such channels could initiate solution of vesicle content. Resultant osmotic swelling might provide some of the impetus for macroscopic membrane contact and discharge It would be interesting to reexamine fracture replicas of synapses, which presumably contain "flattened" synaptic vesicles (Uchizono, 1967 and Bodian, 1970), with this in mind

It may be, however, that markers of membrane fusion, such as the rosette, are not universally present in appropriate faces, and that some of the other details of our fusion hypothesis vary in other cells. It would be surprising if in the long evolutionary history of membrane fusion, with the great divergence of secretory systems, considerable

variability did not arise Nevertheless, the freeze-fracture, freeze-etch technique is obviously a new tool for generating detailed information about membrane fusion in a variety of cells and secretory tissues, and it would also be surprising if many of the features of mucocyst discharge in *Tetrahymena* did not prove to be widely applicable

This work was supported by a grant from the United States Public Health Service (HL 13849)

Received for publication 16 May 1972, and in revised form 15 August 1972.

REFERENCES

AKERT, K., H MOOR, K. PFENNINGER, and C. SANDRI. 1969. Contribution of new impregnation methods and freeze etching to the problems of synaptic fine structure. *Prog. Brain Res.* **31**:223.

ALLEN, R. D. 1967. Fine structure, reconstruction and possible functions of components of the cortex of *Tetrahymena pyriformis*. *J. Protozool.* **14**:553

BODIAN, D. 1970. An electron microscopic characterization of classes of synaptic vesicles by means of controlled aldehyde fixation *J. Cell Biol.* **44**: 115.

BRANTON, D. 1966. Fracture faces of frozen membranes. *Proc Natl Acad. Sci.* U S.A. **55**:1048.

BRESSLAU, E. 1921. Hullenbindung und Gehäusebau bei Protozoan *Mikrokosmos.* **15**:97.

CHALCROFT, J. P., and S. BULLIVANT. 1970 An interpretation of liver cell membrane and junction structure based on observation of freeze-fracture replicas of both sides of the fracture. *J. Cell Biol.* **47**:49.

COHEN, A. L., J. P. MARLOW, and G. E GARNER. 1968. A rapid critical point method using fluorocarbons ("Freons") as intermediate and transitional fluids. *J Microsc. (Paris)* **7**:331.

DEAMER, D. W., and D. BRANTON. 1967. Fracture planes in an ice-bilayer model membrane system. *Science (Wash D C.).* **158**:655.

DEAMER, D. W., R LEONARD, A. TARDIEU, and D. BRANTON. 1970. Lamellar and hexagonal lipid phases visualized by freeze-etching. *Biochim. Biophys. Acta.* **219**:47.

DEL CASTILLO, J., and B. KATZ. 1957. La base "quantale" de la transmission neuromusculaire. *Colloq. Int. Cent. Natl. Rech. Sci.* **67**:245.

ENGSTROM, L. H. 1970. Structure in the erythrocyte membrane. Ph D. Dissertation. University of California, Berkeley.

FRYE, L. D , and M. EDIDIN. 1970. The rapid intermixing of cell surface antigens after formation of mouse-human heterokaryons. *J Cell Sci.* **7**:319.

GILULA, N. B., D. BRANTON, and P. SATIR. 1970 The septate junction· a structural basis for intercellular coupling *Proc. Natl. Acad. Sci U S. A* **67**:213.

GILULA, N B., and P SATIR. 1972. The ciliary necklace. A ciliary membrane specialization. *J. Cell Biol.* **53**:494.

KREUTZIGER, G. O. 1968 Freeze-etching of intercellular junctions of mouse liver Proceedings 26th Meeting of the Electron Microscope Society of America, San Francisco. 234

LEAK, L. V. 1971. Frozen-fractured images of blood capillaries in heart tissue *J. Ultrastruct. Res.* **35**: 127.

LOEWENSTEIN, W. R. 1967. Cell surface membranes in close contact Role of Calcium and Magnesium ions. *J. Colloid Interface Sci.* **25**:34

NANNEY, D. L. 1971. The pattern of replication of cortical units in *Tetrahymena. Dev. Biol* **26**:296

NICKEL, E., and E GRIESHABER. 1969. Elektronenmikroskopische Darstellung der Muskelkapillaren im Gefrierätzbild. *Z. Zellforsch. Mikrosk Anat* **95**:445.

PALADE, G. E., and R. R. BRUNS. 1968. Structural modulation of plasmalemmal vesicles *J. Cell Biol.* **37**:633

PINTO DA SILVA, P. 1972 Translational mobility of the membrane intercalated particles of human erythrocyte ghosts. pH-dependent, reversible aggregation. *J. Cell Biol* **53**:777.

PINTO DA SILVA, P., and D. BRANTON. 1970 Membrane splitting in freeze-etching. *J. Cell Biol* **45**:598.

PITELKA, D R. 1963 Electron Microscopic Structure of Protozoa. Pergamon Press, Inc., New York. 269 pp.

ROBERTSON, J. D. 1959 The ultrastructure of cell membranes and their derivatives. *Biochem. Soc. Symp.* **16**:3.

ROBERTSON, J D. 1972. The structure of biological membranes Current status. *Arch. Intern. Med.* **129**:202.

SATIR, B., and E. R. DIRKSEN 1971. Nucleolar aging in *Tetrahymena pyriformis* during the cultural growth cycle *J. Cell Biol.* **48**:143

SATIR, B., C. SCHOOLEY, and P. SATIR. 1972 *a*. Membrane reorganization during secretion in *Tetrahymena. Nature (Lond)* **235**:53

SATIR, B., C. SCHOOLEY, and P. SATIR. 1972 *b* The ciliary necklace in *Tetrahymena Acta Protozool.* **11**:291.

TILLACK, T. W., and V. T. MARCHESI. 1970. Demonstration of the outer surface of freeze-etched red blood cell membranes. *J Cell Biol.* **45**:649

TOKUYASU, K., and O. H. SCHERBAUM. 1965. Ultrastructure of mucocysts and pellicle of *Tetrahymena pyriformis J. Cell Biol* **27**:67.

UCHIZONO, K. 1967. Inhibitory synapses on the stretch

receptor neurone of the crayfish. *Nature* (*Lond.*). **241**:833.

VAN DEENEN, L. L. M. 1965. Phospholipids and biomembranes. *Prog. Chem. Fats Other Lipids.* **8**:1.

WEHRLI, E., K. MUHLETHALER, and H. MOOR. 1970. Membrane structure as seen with a double replica method for freeze-fracturing. *Exp. Cell Res.* **59**:336.

WILLIAMS, N. E., and O. H. SCHERBAUM. 1959. Morphogenetic events in normal and synchronously dividing *Tetrahymena pyriformis* GL. *J. Embryol. Exp. Morphol.* **7**:241.